

Delbrück and nuclear Rayleigh effects in elastic photon scattering in the giant dipole resonance region

S. Turrini

Dipartimento di Fisica dell'Università di Bologna and Istituto Nazionale di Fisica Nucleare, Sezione di Bologna, I-40126 Bologna, Italy

G. Maino and A. Ventura

Comitato Nazionale per l'Energia Nucleare e le Energie Alternative, I-40138 Bologna, Italy

(Received 11 July 1988)

Elastic photon scattering at the excitation energy of the giant dipole resonance in medium- and heavy-mass nuclei is described by a coherent superposition of Thomson, Delbrück, and nuclear Rayleigh amplitudes, the last being evaluated within the framework of the interacting boson model. New accurate tables of Delbrück amplitudes are also given for $9 \leq E_\gamma \leq 30$ MeV and $0^\circ < \theta < 120^\circ$.

I. INTRODUCTION

Since the introduction of the giant dipole resonance (GDR) (Refs. 1-3) in the interacting boson model (IBM),⁴ calculations of large-angle photon scattering have allowed both good reproduction of experimental data found in the literature^{2,5} and predictions confirmed by the experiment.⁶

In the above-mentioned calculations of elastic scattering the Delbrück contribution had, of course, been neglected. The main purpose of the present work is to describe elastic scattering in the GDR energy range at small and intermediate angles, where the Delbrück amplitude and its interference with the Thomson and Rayleigh amplitudes play a dominant role, and to compare the results with experimental data in the lanthanide and actinide regions, thus extending the range of preliminary calculations, carried out in Ref. 7 for ¹⁶⁸Er. Since the energy region of interest is centered on the giant dipole resonance, the transition amplitudes can be computed in the long-wavelength limit, $R/\lambda \ll 1$, where R is the nuclear radius and λ the wavelength of incident radiation.

II. THE NUCLEAR MODEL

The IBM Hamiltonian describing the excitation of a GDR and its coupling to low-frequency modes has already been discussed in a number of papers.^{1-3,5,8-10} Therefore, the formalism will only be summarized here. The GDR is represented in IBM by a P boson, with spin and parity $J^\pi = 1^-$ and energy $\epsilon_p \cong 77.5 A^{-1/3}$ MeV, interacting with low-energy s and d bosons ($J^\pi = 0^+$ and 2^+ , respectively) according to the following Hamiltonian:

$$\begin{aligned} \hat{H} = & \hat{H}(s,d) + \epsilon_p \hat{n}_p + b_0 [(P^+ \times \bar{P})^{(0)}(d^+ \times \bar{d})^{(0)}]^{(0)} \\ & + b_1 [(P^+ \times \bar{P})^{(1)}(d^+ \times \bar{d})^{(1)}]^{(0)} \\ & + b_2 \{ (P^+ \times \bar{P})^{(2)} [(d^+ \times \bar{s} + s^+ \times \bar{d})^{(2)}] \\ & \quad + \chi_p (d^+ \times \bar{d})^{(2)} \}^{(0)}. \end{aligned} \quad (1)$$

Here, $\hat{H}(s,d)$ is the usual s - d boson Hamiltonian,

whose diagonalization yields the energy spectrum of low-lying collective states of positive parity, χ_p is assumed to have the same value as the corresponding parameter in the quadrupole-quadrupole term of $\hat{H}(s,d)$ (Refs. 4, 5, and 8) and is nearly equal to $-\sqrt{7}/2$ for the prolate nuclear shapes considered in the present work. Finally, b_0 , b_1 , and b_2 are coupling constants to be adjusted on the experimental photoabsorption cross section for a given nucleus or isotope chain. The leading term, responsible for the GDR splitting observed in photoabsorption experiments, is the quadrupole-quadrupole interaction with coefficient b_2 . The boson annihilation operators have the general definition: $\bar{A}_\mu = (-1)^{J+\mu} A_{-\mu}$ ($\mu = -J, \dots, +J$).

The $E1$ transition from the m th low-lying state, $|I_m^+\rangle$, with $I=0,2$, to the n th GDR state, $|1_n^-\rangle$, is given by the reduced matrix element of the dipole operator:^{2,7,8}

$$\hat{D}^{(1)} = D_0(P^+ + P). \quad (2)$$

The GDR widths, $\Gamma_n = \Gamma(E_n)$, cannot be evaluated within the framework of the model and are assumed to depend on the excitation energy, E_n , according to a phenomenological power law:

$$\Gamma(E_n) = k E_n^\gamma, \quad (3)$$

where the k and γ parameters, as well as the dipole operator coefficient, D_0 , and the b coefficients of formula (1) are adjusted so as to give the best fit of the experimental photoabsorption cross section,²

$$\sigma_a(E) = \frac{8\pi e^2}{3\hbar c} E^2 \sum_n \frac{E_n \Gamma_n S_n}{(E_n^2 - E^2)^2 + \frac{\Gamma_n^2}{2} \left[E^2 + E_n^2 + \frac{\Gamma_n^2}{8} \right]}, \quad (4)$$

where E is the incident photon energy and $S_n = |\langle 1_n^- | \hat{D}^{(1)} | 0_1^+ \rangle|^2$ are the dipole strengths.

III. NUCLEAR RAMAN EFFECT

The transition amplitude from the ground state of an even-even nucleus, with $I_i^\pi = 0_1^+$, through GDR excitation, to a final state, $I_f^\pi = 0_k^+$ or 2_k^+ , with emission of a photon of energy $E' = E - E(I_f^\pi)$, which is a kind of nuclear Raman process, is easily expressed by means of the nuclear polarizability, P_J ,¹¹ with $J=0$ or 2 , respectively:

$$P_J = \frac{e^2 \delta_{J I_f}}{[3(2I_f + 1)]^{1/2}} \frac{EE'}{(\hbar c)^2} \times \sum_n \langle I_f^+ \| \hat{D}^{(1)} \| 1_n^- \rangle \langle 1_n^- \| \hat{D}^{(1)} \| 0_1^+ \rangle \times \left[\frac{1}{E_n + E' + i\Gamma_n/2} + \frac{(-1)^J}{E_n - E - i\Gamma_n/2} \right]. \quad (5)$$

In the case of inelastic scattering ($E' < E$), the differential cross section for unpolarized photons is simply

$$\frac{d\sigma_{in}}{d\Omega}(E, E', \theta) = \frac{E'}{E} |P_J|^2 g_J(\theta), \quad (6)$$

where the angular distribution of emitted photons, $g_J(\theta)$, reads

$$g_0(\theta) = (1 + \cos^2\theta)/6, \quad (7a)$$

$$g_2(\theta) = (13 + \cos^2\theta)/12, \quad (7b)$$

when the angular momentum of the final nuclear state is 0 or 2, respectively.

In the case of elastic scattering formula (5), with $J=0$, $I_f^\pi = 0_1^+$ and $E' = E$, reduces to the nuclear Rayleigh amplitude

$$A^R(E) = \frac{1}{\sqrt{3}} P_0 = \frac{E^2}{3(\hbar c)^2} \sum_n S_n \left[\frac{1}{E_n - E - i\Gamma_n/2} + \frac{1}{E_n + E + i\Gamma_n/2} \right], \quad (8)$$

where the factor of $1/\sqrt{3}$ has been introduced for later convenience.

IV. DELBRÜCK EFFECT

The vacuum polarization effect in the elastic scattering of a photon by nuclei, or Delbrück effect, has been studied at the lowest-order Born approximation by a number of authors, in particular De Tollis and co-workers,¹²⁻¹⁴ Papatzakos and Mork,¹⁵ Cheng, Tsai, and Zhou,¹⁶ while higher-order corrections, until now, have been included in the high- E_γ limit;¹⁷ analytical integral representations suitable for numerical evaluation have been given.

Numerical values of Delbrück amplitudes have been tabulated by De Tollis and Luminari¹⁴ at $E_\gamma = 30, 50$, and 70 MeV and by Bar-Noy and Kahane¹⁸ in the $1.33-28$ MeV range: the latter values were given in small energy bins for $E_\gamma \leq 9$ MeV, but were inadequate in the energy regions of our interest. Consequently, it became necessary to obtain new, more accurate results at the energies and scattering angles required.

The two independent complex amplitudes for circularly polarized photons are $a_{++} = a_{--}$ and $a_{+-} = a_{-+}$, defined in the Appendix. Here, the first label refers to incident photon helicity and the second to the scattered one. The differential cross section for pure Delbrück scattering is written in terms of the above-mentioned amplitudes as follows:

$$\frac{d\sigma_{++(+)}(E_\gamma, \theta)}{d\Omega} = (Z\alpha)^4 r_0^2 |a_{++(+)}(E_\gamma, \theta)|^2, \quad (9)$$

TABLE I. Values of $\text{Im } a_{++}$. The Delbrück amplitudes are in units of $(Z\alpha)^2 r_0$; as usual, En denotes 10^n . The energies, E , are in MeV.

| θ deg | $E=9$ | $E=12$ | $E=15$ | $E=18$ | $E=21$ | $E=24$ | $E=27$ | $E=30$ |
|-----------------|---------|---------|---------|---------|---------|---------|---------|---------|
| 0 | 4.71E+0 | 7.76E+0 | 1.12E+1 | 1.49E+1 | 1.88E+1 | 2.30E+1 | 2.74E+1 | 3.19E+1 |
| 1 | 4.16E+0 | 6.01E+0 | 7.58E+0 | 8.75E+0 | 9.74E+0 | 1.05E+1 | 1.09E+1 | 1.14E+1 |
| 2 | 3.27E+0 | 4.23E+0 | 4.82E+0 | 5.19E+0 | 5.35E+0 | 5.45E+0 | 5.42E+0 | 5.39E+0 |
| 5 | 1.60E+0 | 1.71E+0 | 1.69E+0 | 1.64E+0 | 1.59E+0 | 1.53E+0 | 1.47E+0 | 1.40E+0 |
| 10 | 6.37E-1 | 6.19E-1 | 5.90E-1 | 5.55E-1 | 5.24E-1 | 4.97E-1 | 4.75E-1 | 4.48E-1 |
| 20 | 2.07E-1 | 1.94E-1 | 1.79E-1 | 1.66E-1 | 1.54E-1 | 1.42E-1 | 1.33E-1 | 1.25E-1 |
| 30 | 9.79E-2 | 8.98E-2 | 8.15E-2 | 7.43E-2 | 6.80E-2 | 6.27E-2 | 5.78E-2 | 5.39E-2 |
| 40 | 5.49E-2 | 4.94E-2 | 4.42E-2 | 3.95E-2 | 3.58E-2 | 3.32E-2 | 3.03E-2 | 2.80E-2 |
| 50 | 3.33E-2 | 2.95E-2 | 2.61E-2 | 2.34E-2 | 2.11E-2 | 1.92E-2 | 1.76E-2 | 1.61E-2 |
| 60 | 2.12E-2 | 1.86E-2 | 1.64E-2 | 1.46E-2 | 1.32E-2 | 1.19E-2 | 1.08E-2 | 1.00E-2 |
| 70 | 1.40E-2 | 1.22E-2 | 1.07E-2 | 9.41E-3 | 8.52E-3 | 7.69E-3 | 6.99E-3 | 6.41E-3 |
| 80 | 9.45E-3 | 8.14E-3 | 7.11E-3 | 6.26E-3 | 5.65E-3 | 5.04E-3 | 4.60E-3 | 4.24E-3 |
| 90 | 6.52E-3 | 5.59E-3 | 4.86E-3 | 4.32E-3 | 3.79E-3 | 3.43E-3 | 3.12E-3 | 2.85E-3 |
| 100 | 4.40E-3 | 3.79E-3 | 3.28E-3 | 2.85E-3 | 2.56E-3 | 2.30E-3 | 2.09E-3 | 1.91E-3 |
| 110 | 2.96E-3 | 2.52E-3 | 2.18E-3 | 1.94E-3 | 1.72E-3 | 1.55E-3 | 1.41E-3 | 1.29E-3 |
| 120 | 1.97E-3 | 1.68E-3 | 1.45E-3 | 1.27E-3 | 1.12E-3 | 1.02E-3 | 9.34E-4 | 8.44E-4 |

TABLE II. Values of $-Ima_{+-}$. The Delbrück amplitudes are in units of $(Z\alpha)^2 r_0$; as usual, En denotes 10^n . The energies, E , are in MeV. We adopt the definition of the spin-flip amplitude, a_{+-} , given by De Tollis *et al.*, Nuovo Cimento **A32**, 227 (1976) [formula (13)]; therefore, it has the opposite sign with respect to that of Refs. 14 and 15.

| θ deg | $E=9$ | $E=12$ | $E=15$ | $E=18$ | $E=21$ | $E=24$ | $E=27$ | $E=30$ |
|-----------------|-----------|-----------|-----------|-----------|-----------|-----------|-----------|-----------|
| 0 | 0.00 | 0.00 | 0.00 | 0.00 | 0.00 | 0.00 | 0.00 | 0.00 |
| 1 | $9.04E-2$ | $2.15E-1$ | $3.58E-1$ | $5.02E-1$ | $6.40E-1$ | $7.77E-1$ | $9.02E-1$ | $1.03E+0$ |
| 2 | $1.75E-1$ | $3.20E-1$ | $4.58E-1$ | $5.82E-1$ | $6.92E-1$ | $7.89E-1$ | $8.70E-1$ | $9.50E-1$ |
| 5 | $2.42E-1$ | $3.42E-1$ | $4.09E-1$ | $4.56E-1$ | $4.82E-1$ | $5.01E-1$ | $5.06E-1$ | $5.15E-1$ |
| 10 | $2.01E-1$ | $2.30E-1$ | $2.37E-1$ | $2.37E-1$ | $2.32E-1$ | $2.22E-1$ | $2.13E-1$ | $2.06E-1$ |
| 20 | $1.04E-1$ | $1.01E-1$ | $9.36E-2$ | $8.62E-2$ | $7.96E-2$ | $7.37E-2$ | $6.83E-2$ | $6.35E-2$ |
| 30 | $5.99E-2$ | $5.38E-2$ | $4.81E-2$ | $4.35E-2$ | $3.91E-2$ | $3.56E-2$ | $3.24E-2$ | $2.98E-2$ |
| 40 | $3.86E-2$ | $3.36E-2$ | $2.93E-2$ | $2.58E-2$ | $2.31E-2$ | $2.07E-2$ | $1.90E-2$ | $1.74E-2$ |
| 50 | $2.73E-2$ | $2.32E-2$ | $1.99E-2$ | $1.74E-2$ | $1.54E-2$ | $1.38E-2$ | $1.25E-2$ | $1.14E-2$ |
| 60 | $2.07E-2$ | $1.73E-2$ | $1.47E-2$ | $1.27E-2$ | $1.12E-2$ | $1.00E-2$ | $9.04E-3$ | $8.23E-3$ |
| 70 | $1.65E-2$ | $1.36E-2$ | $1.15E-2$ | $9.90E-3$ | $8.69E-3$ | $7.73E-3$ | $6.96E-3$ | $6.33E-3$ |
| 80 | $1.37E-2$ | $1.12E-2$ | $9.43E-3$ | $8.10E-3$ | $7.09E-3$ | $6.30E-3$ | $5.66E-3$ | $5.14E-3$ |
| 90 | $1.16E-2$ | $9.47E-3$ | $7.93E-3$ | $6.79E-3$ | $5.93E-3$ | $5.26E-3$ | $4.72E-3$ | $4.28E-3$ |
| 100 | $1.02E-2$ | $8.26E-3$ | $6.90E-3$ | $5.90E-3$ | $5.15E-3$ | $4.57E-3$ | $4.10E-3$ | $3.71E-3$ |
| 110 | $9.19E-3$ | $7.41E-3$ | $6.17E-3$ | $5.27E-3$ | $4.59E-3$ | $4.07E-3$ | $3.65E-3$ | $3.30E-3$ |
| 120 | $8.41E-3$ | $6.76E-3$ | $5.62E-3$ | $4.80E-3$ | $4.18E-3$ | $3.70E-3$ | $3.32E-3$ | $3.01E-3$ |

where Z is the atomic number, α the fine-structure constant and r_0 the classical electron radius. We have also calculated the Delbrück amplitudes, for the sake of completeness and comparison with the values in literature,^{14,18} in the 9–30 MeV energy range, for scattering angles, θ , ranging from 0° to 120° , with particular care for small angles, where the amplitudes show rapid variations. In Ref. 14 imaginary parts were given as a threefold integral representation [Eq. (3)], while real parts were given [Eqs. (5) and (15)] as a sum of a fourfold integral representation and a subtraction term: the latter, related to the backward scattering amplitude and thus vanishing in the case of $\text{Re } a_{++}$, involves a threefold integration, the inmost one being a principal value.

The formulas of Ref. 14 have been translated into new numerical programs and the integrations performed by

means of a Monte Carlo adaptative subroutine, RIWIAD (Riemann integration with interval adjustment), written by Lautrup¹⁹ and slightly modified in order to permit multiple runs, and the CAUCHY subroutine written by Kölbig²⁰ for the evaluation of principal value integrals. The calculations, carried out on a number of VAX machines at the Department of Physics of Bologna University, required about 450 d CPU time: though this amount of CPU time was shared between several VAX computers available at the department, the calculations required more than a solar year.

In evaluating the scattering amplitudes at $\theta=0^\circ$, use has been made of suitable analytical series.¹³ For the other angles, we follow the method of Ref. 14. The threefold integration in the imaginary parts was carried out in only a few Monte Carlo fast iterations at small angles up to a

TABLE III. Values of $\text{Re } a_{++}$. The Delbrück amplitudes are in units of $(Z\alpha)^2 r_0$; as usual, En denotes 10^n . The energies, E , are in MeV.

| θ deg | $E=9$ | $E=12$ | $E=15$ | $E=18$ | $E=21$ | $E=24$ | $E=27$ | $E=30$ |
|-----------------|-----------|-----------|-----------|-----------|-----------|-----------|-----------|-----------|
| 0 | $5.29E+0$ | $7.48E+0$ | $9.69E+0$ | $1.19E+1$ | $1.42E+1$ | $1.64E+1$ | $1.87E+1$ | $2.09E+1$ |
| 1 | $3.45E+0$ | $3.83E+0$ | $3.99E+0$ | $3.78E+0$ | $3.66E+0$ | $3.65E+0$ | $3.40E+0$ | $3.29E+0$ |
| 2 | $2.36E+0$ | $2.37E+0$ | $2.28E+0$ | $2.03E+0$ | $1.95E+0$ | $1.82E+0$ | $1.66E+0$ | $1.54E+0$ |
| 5 | $9.97E-1$ | $8.33E-1$ | $7.18E-1$ | $6.53E-1$ | $5.92E-1$ | $5.06E-1$ | $4.82E-1$ | $4.18E-1$ |
| 10 | $3.97E-1$ | $3.40E-1$ | $2.67E-1$ | $2.38E-1$ | $2.06E-1$ | $1.91E-1$ | $1.72E-1$ | $1.49E-1$ |
| 20 | $1.41E-1$ | $1.17E-1$ | $9.68E-2$ | $8.57E-2$ | $7.18E-2$ | $6.71E-2$ | $5.83E-2$ | $5.48E-2$ |
| 30 | $7.72E-2$ | $6.32E-2$ | $5.04E-2$ | $4.27E-2$ | $3.81E-2$ | $3.27E-2$ | $3.01E-2$ | $2.79E-2$ |
| 40 | $4.56E-2$ | $3.61E-2$ | $3.16E-2$ | $2.50E-2$ | $2.26E-2$ | $1.87E-2$ | $1.73E-2$ | $1.66E-2$ |
| 50 | $3.04E-2$ | $2.32E-2$ | $1.92E-2$ | $1.72E-2$ | $1.47E-2$ | $1.35E-2$ | $1.12E-2$ | $1.03E-2$ |
| 60 | $2.08E-2$ | $1.54E-2$ | $1.30E-2$ | $1.12E-2$ | $9.78E-3$ | $8.30E-3$ | $7.44E-3$ | $7.17E-3$ |
| 70 | $1.50E-2$ | $9.83E-3$ | $8.75E-3$ | $7.77E-3$ | $7.37E-3$ | $5.79E-3$ | $5.69E-3$ | $4.92E-3$ |
| 80 | $9.35E-3$ | $7.49E-3$ | $6.47E-3$ | $5.50E-3$ | $4.79E-3$ | $4.59E-3$ | $3.72E-3$ | $3.60E-3$ |
| 90 | $6.96E-3$ | $5.97E-3$ | $4.32E-3$ | $3.76E-3$ | $3.51E-3$ | $3.00E-3$ | $2.66E-3$ | $2.50E-3$ |
| 100 | $4.85E-3$ | $3.68E-3$ | $3.43E-3$ | $2.47E-3$ | $2.30E-3$ | $1.98E-3$ | $2.06E-3$ | $1.74E-3$ |
| 110 | $3.32E-3$ | $2.43E-3$ | $2.25E-3$ | $1.96E-3$ | $1.62E-3$ | $1.26E-3$ | $1.30E-3$ | $1.22E-3$ |
| 120 | $2.21E-3$ | $1.58E-3$ | $1.39E-3$ | $1.20E-3$ | $1.08E-3$ | $9.57E-4$ | $9.35E-4$ | $8.08E-4$ |

TABLE IV. Values of $-\text{Re} a_{+-}$. The Delbrück amplitudes are in units of $(Z\alpha)^2 r_0$; as usual En denotes 10^n . The energies E , are in MeV. We adopt the definition of the spin-flip amplitude, a_{+-} , given by De Tollis *et al.*, Nuovo Cimento **A32**, 227 (1976) [formula (13)]; therefore, it has the opposite sign with respect to that of Ref. 14 and 15.

| θ deg | $E=9$ | $E=12$ | $E=15$ | $E=18$ | $E=21$ | $E=24$ | $E=27$ | $E=30$ |
|-----------------|-----------|-----------|-----------|-----------|-----------|-----------|-----------|-----------|
| 0 | 0.00 | 0.00 | 0.00 | 0.00 | 0.00 | 0.00 | 0.00 | 0.00 |
| 1 | $1.26E-1$ | $1.86E-1$ | $2.12E-1$ | $2.09E-1$ | $2.10E-1$ | $2.09E-1$ | $1.92E-1$ | $1.88E-1$ |
| 2 | $1.45E-1$ | $1.66E-1$ | $1.62E-1$ | $1.67E-1$ | $1.51E-1$ | $1.41E-1$ | $1.29E-1$ | $1.30E-1$ |
| 5 | $1.18E-1$ | $1.15E-1$ | $1.04E-1$ | $9.75E-2$ | $9.13E-2$ | $8.54E-2$ | $8.11E-2$ | $7.62E-2$ |
| 10 | $8.52E-2$ | $7.68E-2$ | $6.97E-2$ | $6.14E-2$ | $5.72E-2$ | $5.07E-2$ | $4.33E-2$ | $4.20E-2$ |
| 20 | $4.76E-2$ | $3.92E-2$ | $3.32E-2$ | $2.97E-2$ | $2.58E-2$ | $2.35E-2$ | $2.11E-2$ | $1.92E-2$ |
| 30 | $3.12E-2$ | $2.51E-2$ | $2.14E-2$ | $1.82E-2$ | $1.57E-2$ | $1.37E-2$ | $1.23E-2$ | $1.15E-2$ |
| 40 | $2.23E-2$ | $1.80E-2$ | $1.49E-2$ | $1.25E-2$ | $1.09E-2$ | $9.74E-3$ | $8.68E-3$ | $7.91E-3$ |
| 50 | $1.73E-2$ | $1.38E-2$ | $1.13E-2$ | $9.60E-3$ | $8.30E-3$ | $7.27E-3$ | $6.53E-3$ | $5.91E-3$ |
| 60 | $1.43E-2$ | $1.10E-2$ | $9.06E-3$ | $7.59E-3$ | $6.51E-3$ | $5.84E-3$ | $5.22E-3$ | $4.75E-3$ |
| 70 | $1.20E-2$ | $9.43E-3$ | $7.59E-3$ | $6.29E-3$ | $5.55E-3$ | $5.00E-3$ | $4.42E-3$ | $4.02E-3$ |
| 80 | $1.03E-2$ | $8.04E-3$ | $6.51E-3$ | $5.52E-3$ | $4.77E-3$ | $4.24E-3$ | $3.86E-3$ | $3.76E-3$ |
| 90 | $9.27E-3$ | $7.18E-3$ | $5.78E-3$ | $4.96E-3$ | $4.31E-3$ | $3.84E-3$ | $3.83E-3$ | $3.10E-3$ |
| 100 | $8.50E-3$ | $6.50E-3$ | $5.27E-3$ | $4.49E-3$ | $3.96E-3$ | $4.02E-3$ | $3.11E-3$ | $2.83E-3$ |
| 110 | $7.82E-3$ | $5.98E-3$ | $4.94E-3$ | $4.19E-3$ | $3.67E-3$ | $3.26E-3$ | $2.90E-3$ | $2.62E-3$ |
| 120 | $7.42E-3$ | $5.64E-3$ | $4.65E-3$ | $3.96E-3$ | $3.98E-3$ | $3.05E-3$ | $2.73E-3$ | $2.77E-3$ |

maximum of about 150 iterations in the less favorable cases of large angles for $\text{Im } a_{++}$. On the contrary, the fourfold integration in the real parts required up to thousands of fairly slow iterations, more than 8500 in the less favorable case of large angles for $\text{Re } a_{+-}$, while calculation of the subtraction terms required dozens of very slow iterations. The convergence was checked by chi-square tests of the iteration procedure.

Tables I and II give the values of the imaginary parts, Tables III and IV the real parts with three significant digits. The relative errors of the imaginary parts are equal to or smaller than 1%. Since the real parts are given as sums of an integral representation and of subtraction terms, their relative errors depend on the ratio of the contributions: both subtraction terms have a 1% precision, while integral representations are less accurate. In the complete values of $\text{Re } a_{++}$, where the subtraction terms vanish, relative errors come from the integral representations and are smaller than 5% for $\theta < 60^\circ$, smaller than 10% for larger angles. In the case of $\text{Re } a_{+-}$, where the subtraction terms are present and large, the relative errors are usually 4% at small angles ($\theta < 5^\circ$), 3% or even 2% at intermediate angles (up to 40°), and 1% at large angles, with a few exceptions of 2% in some high- E_γ

cases. The comparison with previous results in Ref. 14 at $E_\gamma = 30$ MeV and Ref. 18 at $E_\gamma = 9$ MeV is satisfactory and within the limits of the computational method. It is worth recalling that the global minus sign of the $\text{Im } a_{+-}$ values given in Table I of Ref. 18 is wrong, once the corresponding real parts are assumed to be positive.

V. ELASTIC SCATTERING CROSS SECTION

Elastic scattering in the GDR region is taken as the coherent superposition of the above-mentioned nuclear Rayleigh and Delbrück effects with the classical Thomson amplitude, written in its simplest form as:

$$A_{\lambda\lambda'}^T = -\frac{Z^2 e^2}{AMc^2} \epsilon_\lambda \cdot \epsilon_{\lambda'}^* \equiv A_0^T \epsilon_\lambda \cdot \epsilon_{\lambda'}^*, \quad (10)$$

where A is the mass number, M the atomic mass unit, ϵ_λ and $\epsilon_{\lambda'}$ the initial and final photon polarization vector, respectively.

Let $A_{\lambda\lambda'}$, with $\lambda, \lambda' = \pm 1$, be the total amplitude of elastic scattering of photons with initial polarization λ and final polarization λ' . The differential cross section for unpolarized photons in the initial and final states is⁷

$$\begin{aligned} \frac{d\sigma_{\text{el}}}{d\Omega}(E_\gamma, \theta) &= \frac{1}{2} \sum_{\lambda\lambda'} |A_{\lambda\lambda'}(E_\gamma, \theta)|^2 \\ &= \frac{1}{2} \sum_{\lambda\lambda'} \{ |A_{\lambda\lambda'}^D(E_\gamma, \theta)|^2 + |A_0^T + A^R(E_\gamma)|^2 [\frac{1}{4}(1 + \cos^2\theta) + \frac{1}{2}\lambda\lambda' \cos\theta] + A_{\text{int}}(\lambda, \lambda'; E_\gamma, \theta) \}. \end{aligned} \quad (11)$$

Here, the Delbrück amplitudes, $A_{\lambda\lambda'}^D$, are connected to the dimensionless quantities, $a_{\lambda\lambda'}$, defined in the previous section and listed in Tables I–IV by the relationship

$$A_{\lambda\lambda'}^D(E_\gamma, \theta) = Z^2 \alpha^2 r_0 a_{\lambda\lambda'}(E_\gamma, \theta). \quad (12)$$

Finally, $A^{\text{int}}(\lambda, \lambda'; E_\gamma, \theta)$ is the interference of the nuclear Rayleigh, Thomson, and Delbrück amplitudes:

$$A^{\text{int}}(\lambda, \lambda'; E_\gamma, \theta) = 2 \{ \text{Re} [A_{\lambda\lambda'}^D(E_\gamma, \theta)] \cdot [A_0^T + \text{Re} A^R(E_\gamma)] + \text{Im} [A_{\lambda\lambda'}^D(E_\gamma, \theta)] \cdot \text{Im} A^R(E_\gamma) \} \cdot d_{-\lambda, -\lambda'}^1(\theta). \quad (13)$$

Here, $d_{-\lambda, -\lambda}^1$ is a Wigner rotation matrix, with elements

$$d_{1,1}^1 = d_{-1,-1}^1 = \cos^2(\frac{1}{2}\theta), \quad (14a)$$

$$d_{1,-1}^1 = d_{-1,1}^1 = \sin^2(\frac{1}{2}\theta). \quad (14b)$$

It has to be pointed out that the elastic scattering cross section defined by formulas (10)–(14) lacks a number of contributions of minor importance in the energy and angular ranges we are interested in, $8 \leq E_\gamma \leq 20$ MeV and $30^\circ \leq \theta \leq 120^\circ$, respectively. For a thorough discussion of a more general form of the elastic cross section, the reader is referred, for instance, to Ref. 22, where an analysis of scattering of 2–10 MeV photons by ^{238}U is carried out, with the addition of an incoherent term to the elastic cross section, due to nuclear resonance fluorescence from bound levels, whose importance decreases with increasing photon energy and becomes negligible in the GDR region. For analogous reasons we have omitted the Rayleigh scattering from atomic electrons in the coherent cross section, because it is important at smaller energies and angles than those considered in the present work.

At higher photon energies different corrections become sizable, for instance, the contribution of other giant resonances, such as isoscalar and isovector quadrupole excitations, to the nuclear Rayleigh amplitude.⁸ The experimental uncertainties of the photoabsorption cross section, on which the nuclear model parameters are adjusted, are, in general, too large for reliable evaluation of the effect of $E2$ giant resonances in the GDR energy region. Moreover, formula (10) for the Thomson amplitude is strictly correct only in the $E_\gamma \rightarrow 0$ limit. At high photon energy, where the long-wavelength approximation on which our formulas are based is no longer valid, a correction due to proton and virtual meson form factors becomes important (see, for instance, Ref. 21). The Thomson contribution to the scattering cross section has the same angular dependence as the nuclear Rayleigh term and, for the nuclei and the energy region considered in the present work, it is always smaller by at least a factor of 3: that is why we have used the classical limit given by formula (10).

VI. RESULTS AND COMMENTS

The scattering formalism discussed in the previous sections has been applied to deformed heavy nuclei, ^{156}Gd , ^{232}Th , and ^{238}U , for which both the low-energy collective states and the giant dipole excitations can be satisfactorily reproduced within the IBM framework. In the case of gadolinium the lowest-order Born approximation to the Delbrück amplitudes is expected to be accurate enough to make Coulomb corrections negligible, owing to the small value of the expansion parameter, $Z\alpha \approx \frac{64}{137}$. This is, of course, more questionable for uranium and thorium, where sizable discrepancies between calculated and experimental scattering cross sections at intermediate angles have been interpreted in terms of Coulomb corrections.^{22–24}

The IBM-Hamiltonian parameters used for the above-

TABLE V. IBM parameters.

| | ^{156}Gd | ^{232}Th | ^{238}U |
|--|-------------------|-------------------|------------------|
| N^a | 12 | 12 | 15 |
| ε_d (MeV) ^a | 0.0 | 0.0 | 0.0 |
| a_0 (MeV) ^a | 0.0060 | −0.0014 | −0.0014 |
| a_1 (MeV) ^a | 0.0046 | 0.0035 | 0.0028 |
| a_2 (MeV) ^a | −0.0162 | −0.0108 | −0.0116 |
| χ^a | −0.9790 | −1.3280 | −1.3230 |
| a_3 (MeV) ^a | 0.0440 | 0.0 | 0.0 |
| a_4 (MeV) ^a | 0.0125 | 0.0 | 0.0 |
| ε_p (MeV) ^b | 14.30 | 12.60 | 12.90 |
| b_0 (MeV) ^b | 0.0 | 0.200 | 0.0 |
| b_1 (MeV) ^b | 0.500 | 0.0 | 0.0 |
| b_2 (MeV) ^b | 0.360 | 0.300 | 0.250 |
| χ_p^b | −0.9790 | −1.3230 | −1.3230 |
| D_0 (fm) ^c | 8.0 | 10.4–11.4 | 10.4–11.4 |
| k (MeV ^{1−γ)^d} | 0.0050 | 0.0065 | 0.0065 |
| γ^d | 2.5 | 2.5 | 2.5 |

^a s - d boson parameters, defined in Ref. 5.

^b P -boson parameters of formula (1).

^cCoefficient of the $E1$ operator in formula (2); for ^{232}Th and ^{238}U see Figs. 5 and 6.

^dParameters of formula (3).

mentioned isotopes are listed in Table V: the s - d boson parameters have been adjusted on the experimental energies and $E2$ transition strengths of low-lying positive-parity states, the P -boson parameters derive from a best fit to the experimental photoabsorption cross sections, taken from Ref. 25 for ^{156}Gd and from Ref. 26 for ^{232}Th and ^{238}U . The experimental and calculated cross sections are shown in Figs. 1–3.

Once the IBM parameters have been adjusted on low-energy levels and photoabsorption data the calculation of scattering cross sections is performed without further degrees of freedom.

The differential cross section for elastic scattering of 12 MeV photons by ^{156}Gd is plotted in Fig. 4 as a function of the scattering angle. The separate contributions of

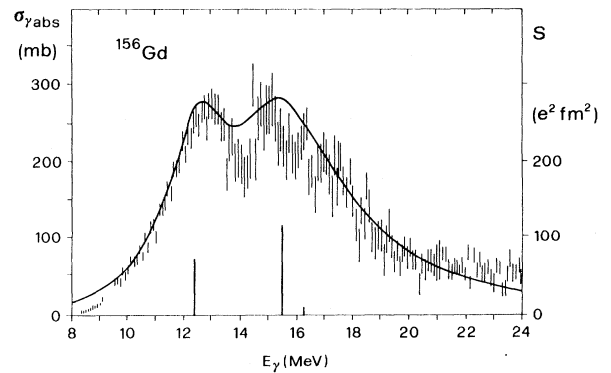


FIG. 1. Photoabsorption cross section by ^{156}Gd . Solid line: present calculations with the parameters of Table V; experimental data are taken from Ref. 25. The straight line segments at the bottom represent the calculated dipole strengths, S_n , in $e^2\text{fm}^2$ units.

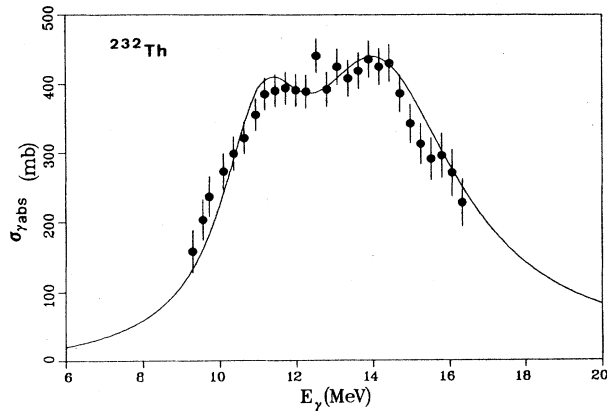


FIG. 2. Photoabsorption cross section by ^{232}Th . Solid line: present calculations with the parameters of Table V ($D_0 = 10.4$ fm); experimental data are taken from Ref. 26.

Thomson, Delbrück, and nuclear Rayleigh effects, as well as the absolute value of the interference term of formula (13), are also plotted as functions of θ . As expected, the pure Delbrück contribution decreases rapidly with increasing θ , but the interference term, linear in the Delbrück amplitudes, is never negligible: being positive at small angles, it causes a sizable increment there of the total cross section; at large angles ($\theta > 80^\circ$) it becomes negative and produces a non-negligible decrement. The nuclear Rayleigh contribution fixes the order of magnitude of the total cross section everywhere except at small angles, where the Delbrück term is dominant.

The elastic scattering of 9 MeV photons by ^{232}Th and ^{238}U is plotted in Figs. 5 and 6, respectively, where the solid and dashed curves correspond to two choices of the D_0 coefficient in the electric dipole operator of formula (2). The lower D_0 value in Table V reproduces the experimental photoabsorption data of Ref. 26, as shown in Figs. 2 and 3, the higher value being compatible with the higher limit of the data²⁷ at $E_\gamma = 9$ MeV. It has to be pointed out that the experimental photoabsorption cross sections for thorium and uranium are affected by large

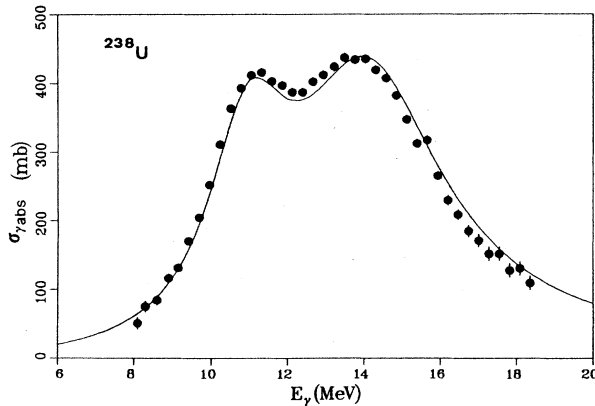


FIG. 3. Photoabsorption cross section by ^{238}U . Solid line: present calculations with the parameters of Table V ($D_0 = 10.4$ fm); experimental data are taken from Ref. 26.

uncertainties in this energy region, as is evident from a comparison of Refs. 26 and 27.

In the case of ^{238}U , the discrepancy between the present calculation and the experimental data confirms the conclusions of Ref. 23, where a similar effect has been interpreted in terms of missing Coulomb corrections to the Delbrück amplitudes. Also the refined analyses carried out in Ref. 22 for ^{238}U and in Ref. 24 for both ^{238}U and ^{232}Th support the conclusion that Coulomb corrections play an important role in the Delbrück scattering of 9 MeV photons by actinides.

The introduction in the present work of a nuclear model for Rayleigh scattering does not improve the agreement between calculations and experiments obtained in Refs. 22–24, where use had been made of Lorentzian fits or optical theorem plus dispersion relations. The present approach proves successful in reproducing large-angle scattering, where the Delbrück effect plays a minor role, but is not negligible thanks to the interference term (13) and inelastic scattering to the 2_1^+ state,⁵ provided that the

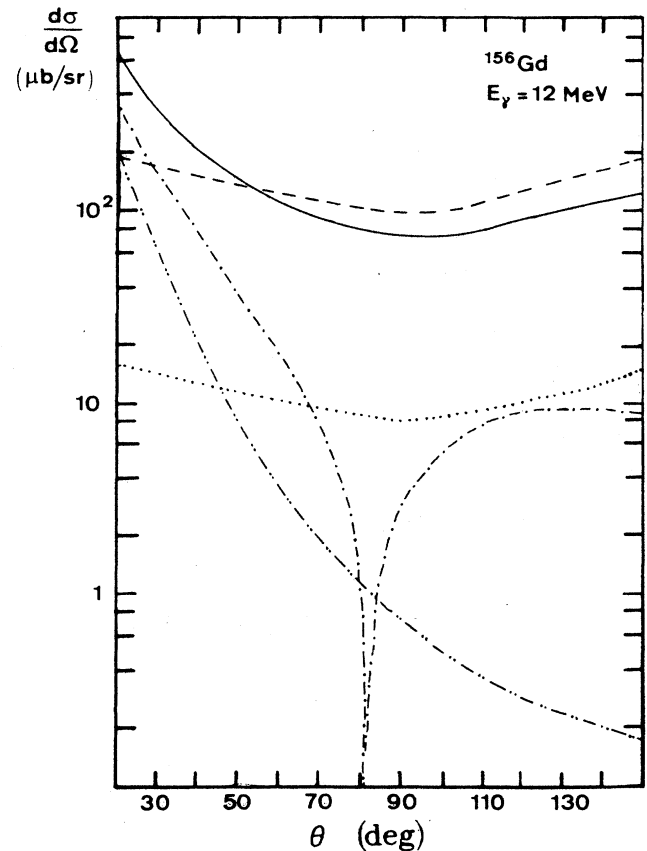


FIG. 4. Differential cross section for elastic scattering of 12 MeV photons by ^{156}Gd . Solid line: calculated total elastic scattering cross section; dashed line: nuclear Rayleigh contribution; dotted line: Thomson contribution; double-dot-dashed line: Delbrück contribution; dot-dashed line: interference term between nuclear Rayleigh, Thomson, and Delbrück amplitudes [formula (13)].

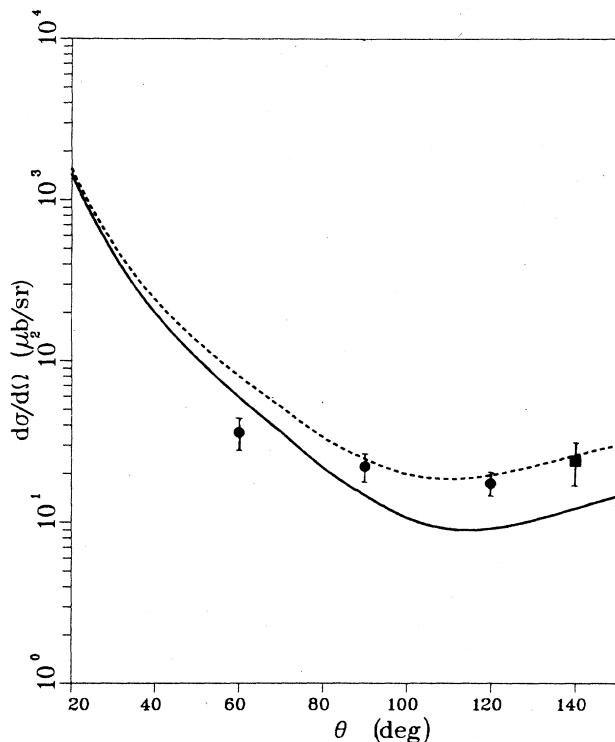


FIG. 5. Differential cross section for elastic scattering of 9 MeV photons by ^{232}Th . Solid line: IBM calculations with $D_0 = 10.4$ fm; dashed line: IBM calculations with $D_0 = 11.4$ fm. Experimental data: ●, Ref. 24; ■, Ref. 29.

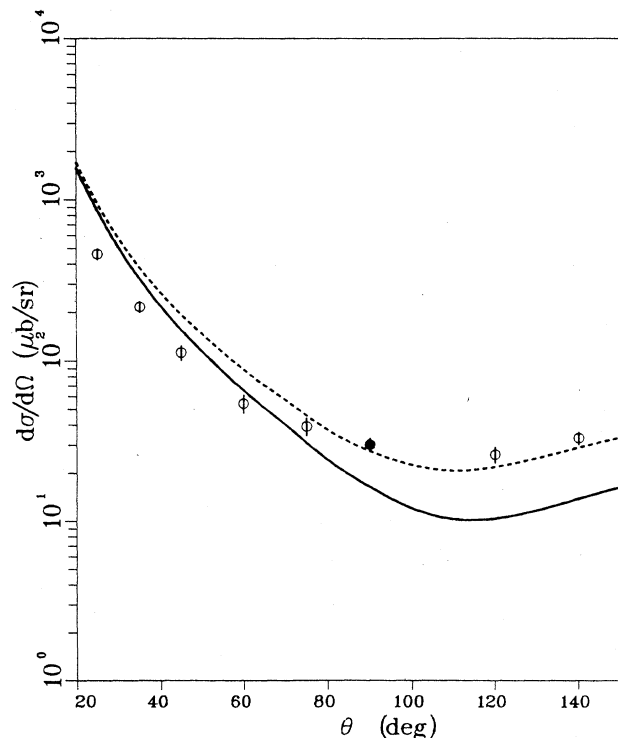


FIG. 6. Differential cross section for elastic scattering of 9 MeV photons by ^{238}U . Solid line: IBM calculations with $D_0 = 10.4$ fm; dashed line: IBM calculations with $D_0 = 11.4$ fm. Experimental data: ●, Ref. 24; ○, Ref. 23.

higher D_0 value of Table V is adopted. While Coulomb corrections apparently are of minor importance in the energy region of 4–7 MeV,²⁸ the situation in the upper tail of the giant dipole resonance is not yet clear and new measurements in the 9–18 MeV range at scattering angles smaller than 90° are desirable in order to throw light on the matter.

It is worth mentioning that in recent measurements of scattering of 25–100 MeV photons by ^{208}Pb in the angular range $\theta = 15^\circ$ – 80° (Ref. 30) the importance of Coulomb corrections is smaller than expected, even at $\theta = 15^\circ$. On the other side, the computational method for Coulomb corrections, based on the impact-factor approximation,¹⁷ has to be carefully reinvestigated, as shown in Ref. 31. In any case, the Delbrück amplitudes tabulated in the present work could be considered a useful supplement of previous calculations.^{14,18}

ACKNOWLEDGMENTS

We are grateful to Professor B. De Tollis and Professor F. Iachello for valuable comments and to Professor L. Luminari for a comparison of numerical techniques in the calculations of Delbrück scattering. The present work has been supported in part by a Ministero della Pubblica Istruzione (MPI) (60%) grant of the Italian Ministry of Education and Sezione di Bologna, INFN.

APPENDIX: DELBRÜCK SCATTERING AMPLITUDES

In this section, the main formulas for Delbrück amplitudes are briefly recalled; they have been originally derived in the lowest perturbative order by De Tollis and co-workers^{12,13} using a dispersion relation at fixed momentum transfer. Therefore, we refer to the original papers^{12,13} for a detailed derivation, while in the following the relevant results are only shown for reader's convenience.

The system of units $\hbar = c = m_e = 1$ is assumed, where m_e is the electron rest mass; the Delbrück scattering is described by means of two independent (complex) amplitudes for circularly polarized photons, namely $a_{++} = a_{--}$ and $a_{+-} = a_{-+}$, labels + and – referring to helicities, the first subscript to the incoming photon (i), the second to the scattered one (o).

The circular polarization states are given by the four-vectors

$$\begin{aligned} (e_{\lambda_i}^{(i)}) &\equiv \left[\frac{1}{\sqrt{2}}(e_1^{(i)} + i\lambda_i e_2^{(i)}), 0 \right], \\ (e_{\lambda_o}^{(o)})^* &\equiv \left[\frac{1}{\sqrt{2}}(e_1^{(o)} - i\lambda_o e_2^{(o)}), 0 \right], \end{aligned} \quad (\text{A1})$$

where λ_i (λ_o) for incoming (outgoing) photon is equal to +1 and –1 for right- and left-handed circular polarization, respectively. Moreover,

$$\begin{aligned} \mathbf{e}_1^{(i)} &= \mathbf{e}_1^{(o)} = (0, 1, 0), \\ \mathbf{e}_2^{(i)} &= (-\cos\frac{1}{2}\theta, 0, -\sin\frac{1}{2}\theta), \\ \mathbf{e}_2^{(o)} &= (-\cos\frac{1}{2}\theta, 0, \sin\frac{1}{2}\theta), \end{aligned} \quad (\text{A2})$$

where θ is the scattering angle.

De Tollis *et al.*^{12,13} give the imaginary parts of Delbrück amplitudes in terms of threefold integrals which contain only irrational and elementary functions of the arguments:

$$\text{Im}a_{++}(d, p) = \frac{1}{\pi p} \int_1^{k^2/4} dy \int_{x_-}^{x_+} dx \int_0^{b(y)} dz A_{\pm}(x, y, z; d, p), \quad k \geq 2, \quad x_{\pm} = [p \pm (k^2 - 4y)^{1/2}]^2, \quad b(y) = \sqrt{1 - 1/y}, \quad (\text{A3})$$

where the kinematical variables, p and d , are defined as follows:

$$\begin{aligned} d &= k \sin\frac{1}{2}\theta, \\ p &= k \cos\frac{1}{2}\theta, \end{aligned} \quad (\text{A4})$$

and k is the photon energy in unit of m_e . If $k \leq 2$ in Eq. (A3), $\text{Im}a_{++}$ vanish.

The real parts of the amplitude are given as subtracted dispersion relations, free from singularities in the fourfold integral representation:

$$\text{Re}a_{++}(d, p) = C_{\pm}(d) + \frac{2p^2}{\pi} P \int_{\alpha(d)}^{\infty} \frac{dp'}{p'} \cdot \frac{D_{\pm}(p', d)}{p'^2 - p^2}. \quad (\text{A5})$$

$$D_{\pm}(p, d) = \frac{1}{\pi p} \int_1^{k^2/4} dy \int_{x_-}^{x_+} dx \int_0^{b(y)} dz \varepsilon(\bar{l}) A_{\pm}(x, y, z; d, p) \quad (k \geq 2), \quad (\text{A6})$$

where $\alpha(d) = (4 - d^2)^{1/2}$ when $d \leq 2$ and $\alpha(d) = 0$ otherwise. The step function, $\varepsilon(x)$, takes the values $\varepsilon(|x|) = 1$, $\varepsilon(-|x|) = -1$, the variable, \bar{l} , being defined later. As usual, P means the principal value of the integral. The A_{\pm} functions in Eqs. (A3), and (A6) are then given by

$$\begin{aligned} A_+(x, y, z; d, p) &= \left[(2y + \mu) \frac{1 + y(z^2 - 1)}{z^2 - 1} \right] R_{01}^{(1)} + \left[-2y \frac{z^2 + 1}{(z^2 - 1)^2} + \frac{2y(\mu - 2)}{z^2 - 1} + y(d^2 - 2d^2y + \mu - 2) \right] R_{02}^{(1)} \\ &+ \left[\frac{2z^2}{(z^2 - 1)^2} - \frac{\mu + d^2}{z^2 - 1} \right] R_{03}^{(1)} - \frac{z^2 + 1}{z^2 - 1} \frac{1}{a_0} + \frac{z^2 + 1}{z^2 - 1} \frac{\bar{l}^2 - r_{12}}{2} k^2 R_{01}^{(1)} \\ &+ \frac{k^2}{y(y + \mu)} \frac{1 + y(z^2 - 1)}{z^2 - 1} \left\{ \left[\frac{r_{12}^2 - \bar{l}^2 r_{12} + \bar{l}^2}{2} \frac{z^2 + 1}{z^2 - 1} + d^2 y (\bar{l}^2 - r_{12}) \right] (R_{02}^{(1)} - R_{12}^{(1)}) \right. \\ &\quad + \frac{\mu - 1}{2} (R_{03}^{(3)} - R_{13}^{(3)}) - \frac{r_{12}}{z^2 - 1} (R_{03}^{(1)} - R_{13}^{(1)}) + r_{12} R_{01}^{(5)} \\ &\quad - \frac{z^4 + 6z^2 + 1}{4y^2(z^2 - 1)^3} (R_{02}^{(4)} - R_{12}^{(4)}) \\ &\quad + \left[\frac{r_{12}(3z^2 + 1)}{y(z^2 - 1)^2} - \frac{1 + 2d^2}{2} \frac{z^2 + 1}{z^2 - 1} \right] (R_{02}^{(2)} - R_{12}^{(2)}) \\ &\quad \left. + \frac{z^2 + 1}{4} (R_{03}^{(4)} - R_{13}^{(4)}) + \frac{z^2}{z^2 - 1} (R_{03}^{(2)} - R_{13}^{(2)}) - R_{01}^{(6)} \right\} \quad (\text{A7}) \end{aligned}$$

and

$$\begin{aligned} A_-(x, y, z; d, p) &= -\frac{1}{a_1} - \left[y - \frac{2\mu + 1}{z^2 - 1} \right] \frac{R_{01}^{(1)}}{2} + d^2 y \frac{1 + y(z^2 - 1)}{y + \mu} \left[r_{12} - \frac{2z^2}{z^2 - 1} \right] \\ &\quad \times \left[R_{02}^{(1)} - R_{12}^{(1)} - \frac{z^2 + 1}{y^2(z^2 - 1)^3} (R_{03}^{(1)} - R_{13}^{(1)}) \right] \\ &\quad + \frac{1}{2} (\bar{l}^2 - r_{12}) k^2 R_{01}^{(1)} + \frac{1}{2} k^2 R_{01}^{(2)} - \frac{k^2}{y(y + \mu)} \frac{1 + y(z^2 - 1)}{z^2 - 1} \\ &\quad \times \left[-\frac{z^2 + 1}{2(z^2 - 1)} (R_{02}^{(3)} - R_{12}^{(3)}) + \frac{(z^2 + 1)^2}{2(z^2 - 1)^2} (R_{03}^{(3)} - R_{13}^{(3)}) + 2y(y + \mu) R_{12}^{(1)} \right. \\ &\quad \left. - \frac{z^2 + 1}{(z^2 - 1)^2} r_{12} (R_{03}^{(1)} - R_{13}^{(1)}) - r_{12} R_{01}^{(5)} \right], \quad (\text{A8}) \end{aligned}$$

where the following variables have been introduced:

$$r_{12} = \frac{x-d^2}{2}, \quad \mu = \frac{x+d^2}{2}, \quad l = x+4y-d^2, \quad (A9)$$

$$\bar{l} = l/2p, \quad \lambda = x - \bar{l}^2,$$

$$a_i = [n_i(n_i - 4d^2\lambda)]^{1/2}, \quad b_{ik} = \frac{c_i + c_k - 4d^2\lambda}{a_i + a_k}, \quad c_i = n_i + a_i \quad (i, k = 0, 1, 2, 3), \quad (A10)$$

$$n_0 = (x+d^2)^2, \quad n_2 = l^2 + 4d^2x + 16d^2y^2(1-z^2), \quad (A11)$$

$$n_1 = (l+2d^2)^2, \quad n_3 = l^2 + 4d^2x + 16d^2(1-z^2)^{-1}.$$

The functions, $R_{ik}^{(s)}$, $s = 1, 2, \dots, 6$, in Eqs. (A7), and (A8) are defined as follows:

$$R_{ik}^{(1)} = \frac{16(b_{ik}-1)}{a_i a_k}, \quad R_{ik}^{(4)} = 16\lambda b_{ik} \left[\frac{\lambda n_i n_k}{c_i^2 c_k^2} - \frac{x}{c_i c_k} \right],$$

$$R_{ik}^{(2)} = \frac{16\lambda b_{ik}}{c_i c_k}, \quad R_{ik}^{(5)} = \frac{\lambda}{2y(y+\mu)} \left[\frac{n_i}{a_i c_i} - \frac{n_k}{a_k c_k} \right] - \frac{4\lambda n_k}{a_k^3}, \quad (A12)$$

$$R_{ik}^{(3)} = \frac{16b_{ik}}{c_i c_k} \left[x + \bar{l}^2 \frac{n_i n_k}{a_i a_k} \right], \quad R_{ik}^{(6)} = \frac{\lambda^2}{4y(y+\mu)} \left[\frac{n_i}{c_i^2} - \frac{n_k}{c_k^2} \right] - \frac{4\lambda^2 n_k}{a_k c_k^2}.$$

Finally, the $C_{\pm}(d)$ functions of Eq. (A5) are related to the backward scattering amplitude,

$$C_{\pm}(d) = (\text{Re} a_{++})_{[k=d, \theta=\pi]}, \quad (A13)$$

$$+-$$

which implies $C_+(d) = 0$ since a_{++} vanishes in the backward direction. Therefore, the only subtraction term to be evaluated is $C_-(d)$, which is expressible by means of a threefold integral.¹⁴

$$C_-(d) = \frac{1}{\pi^2} \int_0^\infty dq \int_{-1}^{+1} d\xi \frac{1}{q^2 + 2d^2 - 2dq\xi} P \int_1^\infty dy \left[\frac{B_1(y, z, \xi; d)}{y-s} + B_2(y, q, \xi; d) \right]. \quad (A14)$$

Moreover, the B_1 and B_2 functions are given by the following expressions:

$$B_1(y, q, \xi; d) = \left[\frac{s_1 s_2}{y_1 y_2} - \frac{2y s_1 s_2}{r y_1 y_2} - \frac{y^2 (s_1^2 + s_2^2)}{y_1^2 y_2^2} \right] b(y) + \left[\frac{4u}{r^2} - \frac{r}{y_1 y_2} + \frac{y(s_1^2 + s_2^2)}{y_1^2 y_2^2} \right] \text{arcosh} \sqrt{y}$$

$$+ \frac{s-r}{r y a'_1} \ln \left[\frac{a'_1 + b(y)}{a'_1 - b(y)} \right] - \left[\frac{2u}{r^2} + \frac{u}{r u'} \right] \frac{1}{a'_2} \ln \left[\frac{a'_2 + b(y)}{a'_2 - b(y)} \right], \quad (A15)$$

$$B_2(y, q, \xi; d) = \left[-\frac{r}{2y_1 y_2} + \frac{r y^2}{y_1^2 y_2^2} + \frac{y(\mu_1 - \mu_2)^2}{2y_1^2 y_2^2} \right] b(y)$$

$$+ \left[-\frac{2r y}{y_1 y_2 u'} - \frac{r y}{y_1^2 y_2^2} - \frac{(\mu_1 - \mu_2)^2}{2y_1^2 y_2^2} - \frac{r}{y^2 (y-r)} \right] \text{arcosh} \sqrt{y} - \frac{1}{u' a'_1} \ln \left[\frac{a'_1 + b(y)}{a'_1 - b(y)} \right], \quad (A16)$$

where the relevant quantities on the right-hand side are defined as follows:

$$4s = 4t = -q_1^2 - q_2^2 - q_3'^2 + 2dq_3', \quad 4\mu_2 = q_1^2 + q_2^2 + q_3'^2 + 4d^2 - 4dq_3', \quad q_3' = q_3 + d, \quad r = -d^2,$$

$$4\mu_1 = q_1^2 + q_2^2 + q_3'^2, \quad 4u = v = -d^2(q_1^2 + q_2^2), \quad s_{1,2} = s + \mu_{1,2}, \quad y_{1,2} = y + \mu_{1,2}, \quad u' = u - (y-s)^2. \quad (A17)$$

$$a'_1 = (1 + u'/r y^2)^{1/2}, \quad a'_2 = (1 + r/u')^{1/2}, \quad b(y) = (1 - 1/y)^{1/2}, \quad q^2 = q_1^2 + q_2^2 + q_3^2.$$

It is worth recalling that the forward scattering amplitude has been also derived by De Tollis¹³ as infinite but rapidly convergent analytical series. In the photon energy range that we have considered ($E_\gamma > 2m_e$), the following formulas hold:

$$\text{Re}a_{++} = \frac{7}{9p} - \frac{9}{4} + \frac{p}{2} \left[\left(\ln \frac{4}{p} \right)^2 - \ln \frac{4}{p} + 3 \right] - \frac{p^2}{9} - \sum_{n=1}^{\infty} \left[\frac{(2n-1)!!}{(2n+2)!!} \right]^2 \frac{4n^3 - n^2 + n - 1}{n^2(2n-1)^2} p^{2n+1}, \quad (\text{A18})$$

$$\begin{aligned} \text{Im}a_{++} = & \frac{14}{9\pi p} \left[\ln \frac{4}{p} - \frac{109}{42} \right] + \frac{p}{\pi} \left[\frac{1}{3} \left(\ln \frac{4}{p} \right)^3 - \frac{1}{2} \left(\ln \frac{4}{p} \right)^2 + \left(3 - \frac{\pi^2}{6} \right) \ln \frac{4}{p} - \frac{7}{4} + \frac{\pi^2}{12} + \zeta(3) \right] \\ & - \frac{2}{\pi} \sum_{n=1}^{\infty} \left[\frac{(2n-1)!!}{(2n+2)!!} \right]^2 \frac{4n^3 - n^2 + n - 1}{n^2(2n-1)^2} p^{2n+1} \\ & \times \left[\ln \frac{4}{p} - \sum_{k=1}^n \frac{1}{k(2k-1)} \frac{12n^2 - 2n + 1}{2(4n^3 - n^2 + n - 1)} + \frac{6n^2 + 2n - 1}{n(n+1)(2n-1)} \right] \end{aligned}$$

($p \leq 1$, $\zeta(3) \approx 1.202\,056\,903$),

(A19)

where $p = 2m_e/E_\gamma$.

- ¹I. Morrison and J. Weise, *J. Phys. G* **8**, 687 (1982).
²F. G. Scholtz and F. J. W. Hahne, *Phys. Lett.* **123B**, 147 (1983).
³D. J. Rowe and F. Iachello, *Phys. Lett.* **130B**, 231 (1983).
⁴For a recent review see, A. Arima and F. Iachello, *Adv. Nucl. Phys.* **13**, 139 (1984).
⁵G. Maino, A. Ventura, L. Zuffi, and F. Iachello, *Phys. Lett.* **152B**, 17 (1985).
⁶A. M. Nathan, in *Nuclear Structure, Reactions and Symmetries*, edited by R. A. Meyer and V. Paar (World-Scientific, Singapore, 1986), Vol. I, p. 385.
⁷S. Turrini, G. Maino, and A. Ventura, in *Nuclear Structure, Reactions and Symmetries*, Ref. 6, p. 397.
⁸G. Maino, A. Ventura, P. Van Isacker, and L. Zuffi, *Phys. Rev. C* **33**, 1089 (1986).
⁹F. G. Scholtz and F. J. W. Hahne, *Phys. Rev. C* **34**, 693 (1986).
¹⁰F. G. Scholtz and F. J. W. Hahne, *Nucl. Phys.* **A471**, 545 (1987).
¹¹J. M. Eisenberg and W. Greiner, *Nuclear Theory II: Excitation Mechanisms of the Nucleus* (North-Holland, Amsterdam, 1970), p. 111.
¹²B. De Tollis, *Nuovo Cimento* **32**, 757 (1964); **35**, 1182 (1965); B. De Tollis, V. Costantini, and G. Pistoni, *ibid.* **A2**, 733 (1971); B. De Tollis, M. Lusignoli, and G. Pistoni, *ibid.* **A32**, 227 (1976); B. De Tollis and G. Pistoni, *ibid.* **A42**, 499 (1977).
¹³B. De Tollis, *Nuovo Cimento* **A72**, 197 (1982).
¹⁴B. De Tollis and L. Luminari, *Nuovo Cimento* **A81**, 633 (1984).
¹⁵P. Papatzakos and K. Mork, *Phys. Rep.* **21**, 81 (1975).
¹⁶H. Cheng, E. Tsai, and X. Zhou, *Phys. Rev. D* **26**, 908 (1982).
¹⁷H. Cheng and T. T. Wu, *Phys. Rev. D* **5**, 3077 (1972).
¹⁸T. Bar-Noy and S. Kahane, *Nucl. Phys.* **A288**, 132 (1979).
¹⁹B. Lautrup, CERN Computer Center Program Library, subroutine D114 (1983).
²⁰K. S. Kölbig, CERN Computer Center Program Library, subroutine D104 (1983).
²¹M. Sanzone-Arenhövel, K. P. Schelhaas, and B. Ziegler, in *Intermediate Energy Nuclear Physics*, edited by R. Bergère, S. Costa, and C. Schaerf (World-Scientific, Singapore, 1982), p. 291.
²²P. Rullhusen, U. Zurmühl, W. Mückenheim, F. Smend, and M. Schumacher, *Nucl. Phys.* **A382**, 79 (1982).
²³S. Kahane and R. Moreh, *Nucl. Phys.* **A308**, 88 (1978).
²⁴P. Rullhusen, U. Zurmühl, F. Smend, M. Schumacher, H. G. Börner, and S. A. Kerr, *Phys. Rev. C* **27**, 559 (1983).
²⁵T. J. Boal, E. G. Muirhead, and D. J. S. Findlay, *Nucl. Phys.* **A406**, 257 (1983).
²⁶A. Veysseyre, H. Beil, R. Bergère, P. Carlos, A. Leprêtre, and K. Kernbath, *Nucl. Phys.* **A199**, 45 (1973).
²⁷T. Caldwell, E. J. Dowdy, B. L. Berman, R. A. Alvarez, and P. Meyer, *Phys. Rev. C* **21**, 1215 (1980).
²⁸M. Schumacher, F. Smend, W. Mückenheim, P. Rullhusen, and H. G. Börner, *Z. Phys. A* **300**, 193 (1981); M. Schumacher, P. Rullhusen, F. Smend, W. Mückenheim, and H. G. Börner, *Nucl. Phys.* **A346**, 418 (1980).
²⁹M. Hass, R. Moreh, and D. Salzmänn, *Phys. Lett.* **36B**, 68 (1971).
³⁰A. Baumann, P. Rullhusen, K. W. Rose, M. Schumacher, J. M. Henneberg, N. Wieloch-Laufenberg, and B. Ziegler, in *Capture Gamma-Ray Spectroscopy, 1987* (IOP, Bristol, 1988), p. 804.
³¹P. Rullhusen, J. Trube, A. Baumann, K. W. Rose, F. Smend, and M. Schumacher, *Phys. Rev. D* **36**, 733 (1987).